

1 Quantifying dynamic facial expressions under naturalistic conditions

2
3 **Authors:** Jayson Jeganathan MBBS^{1,2}, Megan Campbell PhD^{1,2}, Matthew Hyett³, Gordon
4 Parker⁴, Michael Breakspear PhD^{1,2,5}

5 1. School of Psychology, College of Engineering, Science and the Environment,
6 University of Newcastle, Newcastle, NSW, Australia
7 2. Hunter Medical Research Institute, Newcastle, NSW, Australia
8 3. School of Psychological Sciences, University of Western Australia, Crawley, WA,
9 Australia
10 4. School of Psychiatry, University of New South Wales, Kensington, NSW, Australia
11 5. School of Medicine and Public Health, College of Medicine, Health and Wellbeing,
12 University of Newcastle, Newcastle, NSW, Australia

13
14

15 **Contact details**

16 Dr Jayson Jeganathan (corresponding author)
17 HMRI Imaging, Hunter Medical Research Institute
18 Lot 1 Kookaburra Circuit, New Lambton Heights, NSW 2305, Australia
19 Jayson.jeganathan@gmail.com

20
21 Dr Megan Campbell
22 HMRI Imaging, Hunter Medical Research Institute
23 Lot 1 Kookaburra Circuit, New Lambton Heights, NSW 2305, Australia
24 megan.ej.campbell@gmail.com

25
26 Matthew Hyett
27 School of Psychological Sciences
28 35 Stirling Highway
29 University of Western Australia
30 Perth, WA 6009, Australia
31 matthewhyett@gmail.com

32
33 Professor Gordon Parker

34 School of Psychiatry
35 Level 1, AGSM Building
36 University of New South Wales
37 Kensington, NSW 2052, Australia
38 g.parker@unsw.edu.au

39
40 Professor Michael Breakspear
41 HMRI Imaging, Hunter Medical Research Institute
42 Lot 1 Kookaburra Circuit, New Lambton Heights, NSW 2305, Australia
43 mjbreaks@gmail.com

44
45 **Author Contributions**

46 JJ, MC and MB conceptualised the study design. MH and GB collected the melancholia
47 dataset. JJ performed data analysis and drafted the manuscript. JJ, MC, MH, GP, and MB
48 edited the manuscript and approved the final version for submission.

49
50 **Competing Interests statement**
51 We declare no competing interests.

52
53
54 **Key words:**
55 Facial expression, facial affect, naturalistic, FACS, hidden Markov model, major depressive
56 disorder, melancholic depression
57

58

59 **Abstract**

60

61 Facial affect is expressed dynamically – a giggle, grimace, or an agitated frown. However,
62 the characterization of human affect has relied almost exclusively on static images. This
63 approach cannot capture the nuances of human communication or support the naturalistic
64 assessment of affective disorders. Using the latest in machine vision and systems modelling,
65 we studied dynamic facial expressions of people viewing emotionally salient film clips. We
66 found that the apparent complexity of dynamic facial expressions can be captured by a small
67 number of simple spatiotemporal states - composites of distinct facial actions, each expressed
68 with a unique spectral fingerprint. Sequential expression of these states is common across
69 individuals viewing the same film stimuli but varies in those with the melancholic subtype of
70 major depressive disorder. This approach provides a platform for translational research,
71 capturing dynamic facial expressions under naturalistic conditions and enabling new
72 quantitative tools for the study of affective disorders and related mental illnesses.

73

74

75

76 **Introduction**

77

78 Facial expressions are critical to interpersonal communication and offer a nuanced, dynamic
79 and context-dependent insight into internal mental states. Humans use facial affect to infer
80 personality, intentions and emotions, and it is an important component of the clinical
81 assessment of psychiatric illness. For these reasons, there has been significant interest in the
82 objective analysis of facial affect(1–3). However, decisive techniques for quantifying facial
83 affect under naturalistic conditions remain elusive.

84

85 A traditional approach is to count the occurrences of a discrete list of “universal basic
86 emotions”(4). While the most commonly used system designates six basic emotions, there is
87 disagreement about the number and nature of such affective “natural forms” (5,6).
88 Quantifying facial affect using the Facial Action Coding System (FACS), has become the
89 dominant technique to operationalise facial expressions (7). Action units, each corresponding
90 to an anatomical facial muscle group, are rated on a quantitative scale. Traditional emotion
91 labels are associated with the co-occurrence of a specific set of action units – for example a
92 “happy” facial expression corresponds to action units “Cheek Raiser” and “Lip Corner
93 Puller”(8). However, due to the time-intensive nature of manually coding every frame in a
94 video, FACS has traditionally been applied to the analysis of static pictures rather than videos
95 of human faces.

96

97 Recent developments in machine learning have automated the identification of basic
98 emotions and facial action units from images and videos of human faces. Feature extraction
99 for images include local textures (9,10) and 3D geometry(11,12), while video analysis
100 benefits from temporal features such as optical flow(13). Supervised learning algorithms
101 classifying facial expressions based on feature values have achieved impressive accuracies
102 benchmarked to manually coded datasets (see 14 for a review).

103

104 Videos of faces can now be reliably transformed into action unit time series which capture
105 the rich temporal dynamics of facial expressions(11). This is important because human faces
106 express emotional states dynamically – such as in a giggle or a sob. However, the rich
107 potential of these temporal dynamics has not yet been fully exploited in the psychological and

108 behavioural sciences. For example, some psychological studies and databases have asked
109 responders to pose discrete emotions such as happiness or sadness(15). This strategy suits the
110 needs of a classic factorial experimental design but fails to produce the natural dynamics of
111 real-world facial expressions. To evoke dynamic emotion, clinical interviews have been
112 used(16), or participants have been asked to narrate an emotive story or been shown emotive
113 pictures rather than videos(17). Such pictures can be grouped into distinct categories and
114 presented repetitively in a trial structure, but their ecological validity is unclear.
115 Consequently, there is an expanding interest in naturalistic video stimuli such as movie
116 clips(18–20). These are more ecologically valid, have greater test-retest reliability than
117 interviews, evoke stronger facial expressions than static pictures, and produce stronger
118 cortical responses during functional neuroimaging(3,21,22). However, interpreting the facial
119 expressions resulting from naturalistic stimulus viewing poses challenges, because each time
120 point is unique. There is currently no obvious way to parse the stimulus video into discrete
121 temporal segments. Naïve attempts at dimensionality reduction – for example, averaging
122 action unit activations across time – omit temporal dynamics and so fail to capture the
123 complexity of natural responses.

124
125 Disturbances in facial affect occur across a range of mental health disorders, including major
126 depressive disorder, schizophrenia, and dementia. Capturing the nuances of facial affect is a
127 crucial skill in clinical psychiatry but in the absence of quantitative tests this remains
128 dependent on clinical opinion. Supervised learning has shown promise in distinguishing
129 people with major depression from controls, using input features such as facial action units
130 coded manually(23) or automatically(24), or model-agnostic representations of facial
131 movements such as the ‘Bag of Words’ approach(25,26). Studies documenting action unit
132 occurrence during the course of a naturalistic stimulus(27), a short speech(28) or a clinical
133 interview(29), have demonstrated that depression is associated with reduced frequency of
134 emotional expressions, particularly expressions with positive valence. Unfortunately, by
135 averaging action unit occurrence over time, these methods poorly operationalise the
136 clinician’s gestalt sense of affective reactivity, which derive from a patient’s facial responses
137 across a range of contexts.

138
139 Here, we present a novel pipeline for processing facial expression data recorded while
140 participants view a dynamic naturalistic stimulus. The approach is data-driven, eschewing the
141 need to preselect emotion categories or segments of the stimulus video. We derive a time-

142 frequency representation of facial movement information, on the basis that facial movements
143 in vivo are fundamentally dynamic and multiscale. These time-frequency representations are
144 then divided into discrete packets with a hidden Markov model (HMM), a method for
145 inferring hidden states and their transitions from noisy observations. We find dynamic
146 patterns of facial behaviour which are expressed sequentially and localised to specific action
147 units and frequency bands. These patterns are context-dependent, consistent across
148 participants, and correspond to intuitive concepts such as giggling and grimacing. We first
149 demonstrate the validity of this approach on an open-source dataset of facial responses of
150 healthy adults watching naturalistic stimuli. We then test this approach on facial videos of
151 participants with melancholic depression, a severe mood disorder characterised by
152 psychomotor changes(30). We show that dynamic facial patterns reveal specific changes in
153 melancholia, including reduced facial activity in response to emotional stimuli, anomalous
154 facial responses inconsistent with the affective context, and a tendency to get “stuck” in
155 negatively valenced states. Moreover, using these decoded patterns improves accuracy in
156 classifying patients from healthy controls.

157

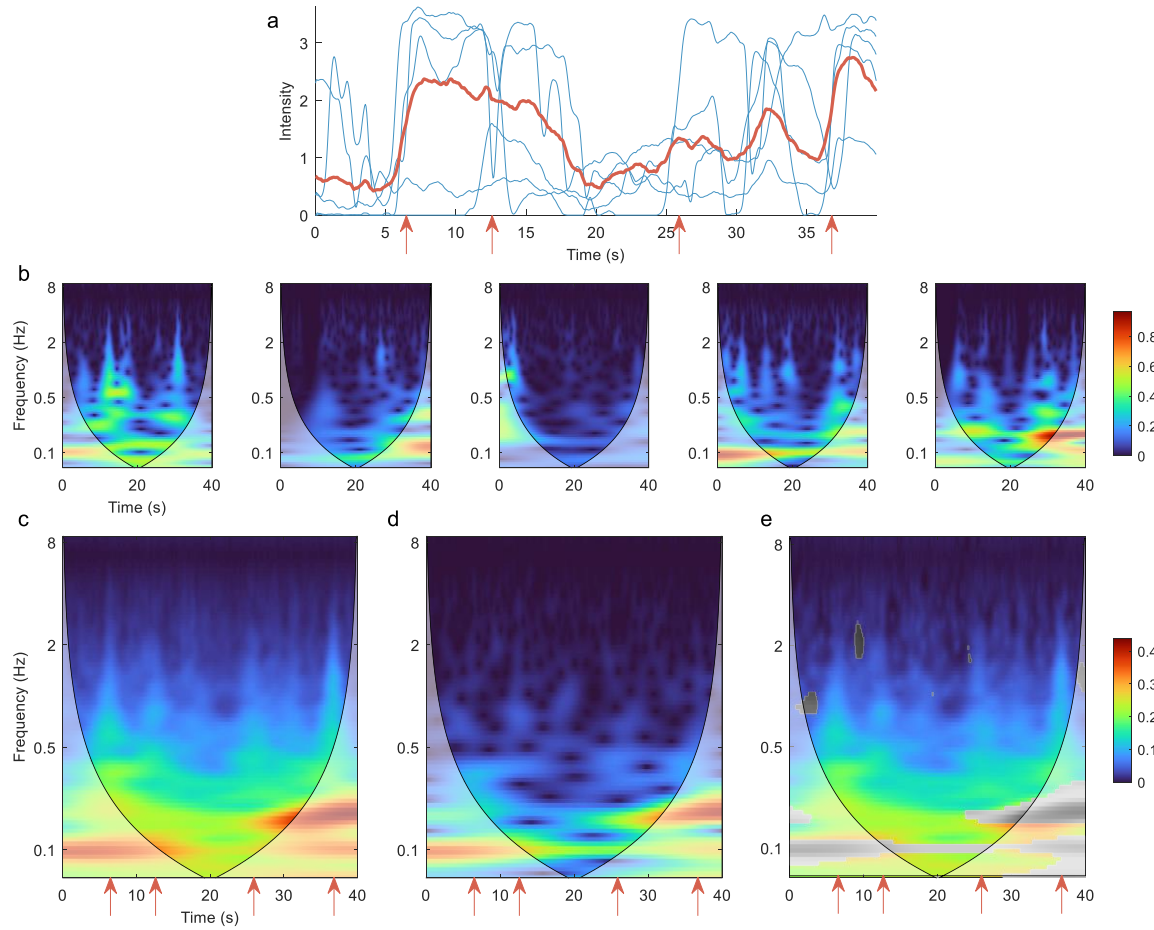
158 **Results**

159 We first analysed dynamic facial expressions from video recordings of 27 participants
160 viewing short emotive clips of 4 minute duration, covering a breadth of basic emotions (the
161 DISFA dataset(19), detailed in Supplementary Table 1). Frame-by-frame action unit
162 activations were extracted with OpenFace software(31) (see Supplementary Table 2 for
163 action unit descriptions).

164

165 From these data, we used the continuous wavelet transform to extract a time-frequency
166 representation of individual action unit time series in each participant. To test whether this
167 time-frequency representation captures high frequency dynamic content, we first compared
168 the group average of these individual time-frequency representations with the time-frequency
169 representation of the group mean time series. We selected the activity of action unit 12 “Lip
170 Corner Puller” during a positive valence video clip (a ‘talking dog’), as this action unit is
171 conventionally associated with happy affect, and its high frequency activity denotes smiling
172 or laughing. Compared to the group mean time series, the time series of individuals had
173 significantly greater amplitude (Figure 1a), particularly at higher frequencies (Figure 1e).
174 This demonstrates that the time-frequency representations of individual participants capture
175 high frequency dynamics that are obscured by characterising group-averaged time courses.
176 This is because stimulus-evoked facial action unit responses have asynchronous alignment
177 across participants, hence cancelling when superimposed. This problem is avoided in the
178 group-level time-frequency representation, whereby the amplitude is first extracted at the
179 individual level, prior to group averaging. Comparable results occurred in all action units
180 (Supplementary Figure 2).

181



182

183 **Figure 1.** Time-frequency representation of action unit 12 “Lip Corner Puller” during
184 positive valence video stimulus reveals high frequency dynamics. (a) Action unit time series
185 for 5 example participants (blue). The group mean time course across all participants is
186 shown in red. Red arrows indicate funny moments in the stimulus, evoking sudden facial
187 changes in individual participants. These changes are less prominent in the group mean time
188 course. (b) Time-frequency representation for the same 5 participants, calculated as the
189 amplitude of the continuous wavelet transform. Shading indicates the cone of influence – the
190 region contaminated by edge effects. (c) Mean of all participants’ time-frequency
191 representations. (d) Time-frequency representation of the group mean time course. Red
192 arrows correspond to time points with marked high frequency activity above 1 Hz. (e)
193 Difference between (c) and (d). Non-significant differences ($p > 0.05$) are shown in
194 greyscale. Common colour scale is used for (c)-(e).

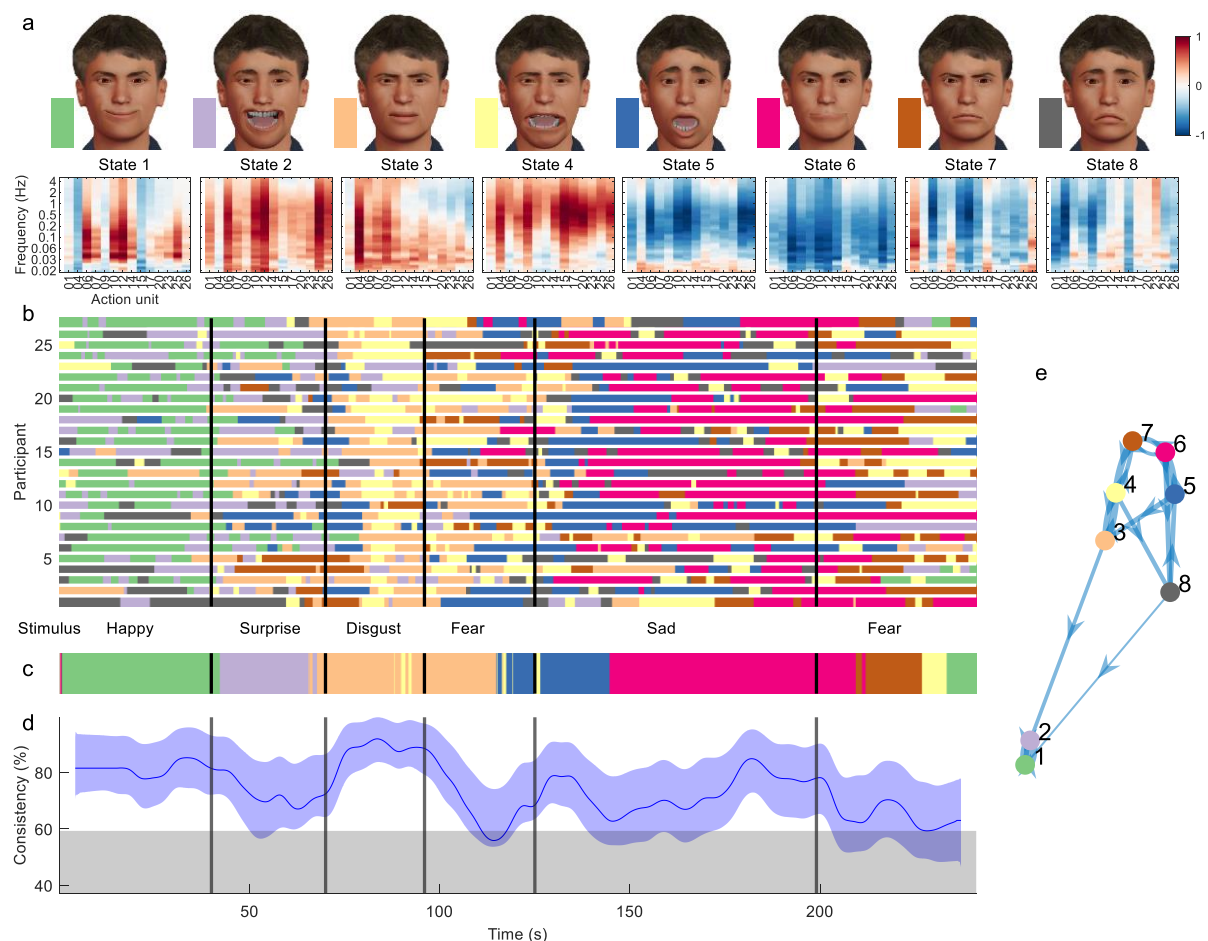
195

196

197 Having shown how the time-frequency representation captures dynamic content, we next
198 sought to quantify the joint dynamics of facial action units. To this end, a hidden Markov
199 model (HMM) was inferred from the time course of all facial action units' time-frequency
200 representations. A HMM infers a set of distinct states from noisy observations, with each
201 state expressed sequentially in time according to state-to-state transition probabilities. Each
202 state has a distinct mapping onto the input space, here the space of frequency bands and
203 action units (Figure 2a). Examples of participants in each state are provided in the
204 Supplementary Videos. Their occurrence corresponded strongly with annotated video clip
205 valence (Figure 2b). We found that inferred state sequences had high between-subject
206 consistency, exceeding chance level across the vast majority of time points and reaching 93%
207 during specific movie events (Figure 2d). States were frequency-localised and comprised
208 intuitive combinations of action units which reflected not only distinct emotion categories as
209 defined in previous literature(8), but also stimulus properties such as mixed emotions. State
210 transition probabilities appeared clustered by valence rather than frequency, such that
211 frequent transitions between low and high frequency oscillations of the same facial action
212 units were more likely than transitions between different emotions (Figure 2e).

213

- 214 • States 1 and 2 were active during stimuli annotated as “happy”. They activated two action
215 units typically associated with happiness, action unit 6 “Cheek Raiser” and 12 “Lip
216 Corner Puller”, but also action unit 25 “Lips Part”. State 2 likely represents laughing or
217 giggling as it encompassed high frequency oscillations in positive valence action units, in
218 comparison to the low frequency content of State 1.
- 219 • States 3 and 4 were active during videos evoking fear and disgust – for example of a man
220 eating a beetle larva. They encompassed mixtures of action units conventionally
221 implicated in disgust and fear, at low and high frequency bands respectively. State 3
222 recruited action units 4 “Brow Lowerer” and 9 “Nose Wrinkler”, while state 4 involved
223 these action units as well as action units 15 “Lip Corner Depressor”, 17 “Chin Raiser”,
224 and 20 “Lip Stretcher”.
- 225 • States 5 and 6 occurred predominantly during negatively valenced clips, and deactivated
226 oscillatory activity in most action units, with sparing of action units typically associated
227 with sadness, 4 “Brow Lowerer” and 15 “Lip Corner Depressor”.



228

229 **Figure 2.** Dynamic facial states inferred from time-frequency representation of DISFA
 230 dataset. (a) Mean of the observation model for each state, showing their mapping onto action
 231 units and frequency bands. Avatar faces (top row) for each state show the relative
 232 contribution of each action unit, whereas their spectral projection (bottom row) shows their
 233 corresponding dynamic content. (b) Sequence of most likely states for each participant at
 234 each time point. Vertical lines demarcate transition between stimulus clips with different
 235 affective annotations. (c) Most common states across participants, using a 4s sliding temporal
 236 window. (d) Proportion of participants expressing the most common state. Blue shading
 237 indicates 5% - 95% bootstrap confidence bands for the estimate. Grey shading indicates the
 238 95th percentile for the null distribution, estimated using time-shifted surrogate data. (e)
 239 Transition probabilities displayed as a weighted graph. Each node corresponds to a state.
 240 Arrow thickness indicates the transition probability between states. For visualization clarity,
 241 only the top 20% of transition probabilities are shown. States are positioned according to a
 242 force-directed layout where edge length is the inverse of the transition probability.

243

244 Facial affect in melancholia

245 We next analysed facial video recordings from a cohort of participants with melancholic
 246 depression and healthy controls who watched three video clips consecutively – a stand-up

247 comedy, a sad movie clip and an amusing video (weather report) in a non-English language
248 (German). These three stimuli were chosen from a database of independently rated videos of
249 high salience(32). The stand-up comedy comprises episodic jokes with a deadpan delivery
250 and audience laughter, whereas the weather report depicts someone laughing uncontrollably
251 and spontaneously. Clinical participants with melancholia were recruited from a tertiary
252 mood disorders clinic and met melancholia criteria including psychomotor changes,
253 anhedonia and diurnal mood variation (see Methods). We conducted analyses based firstly on
254 group-averaged time courses, and then on the time-frequency representation.

255

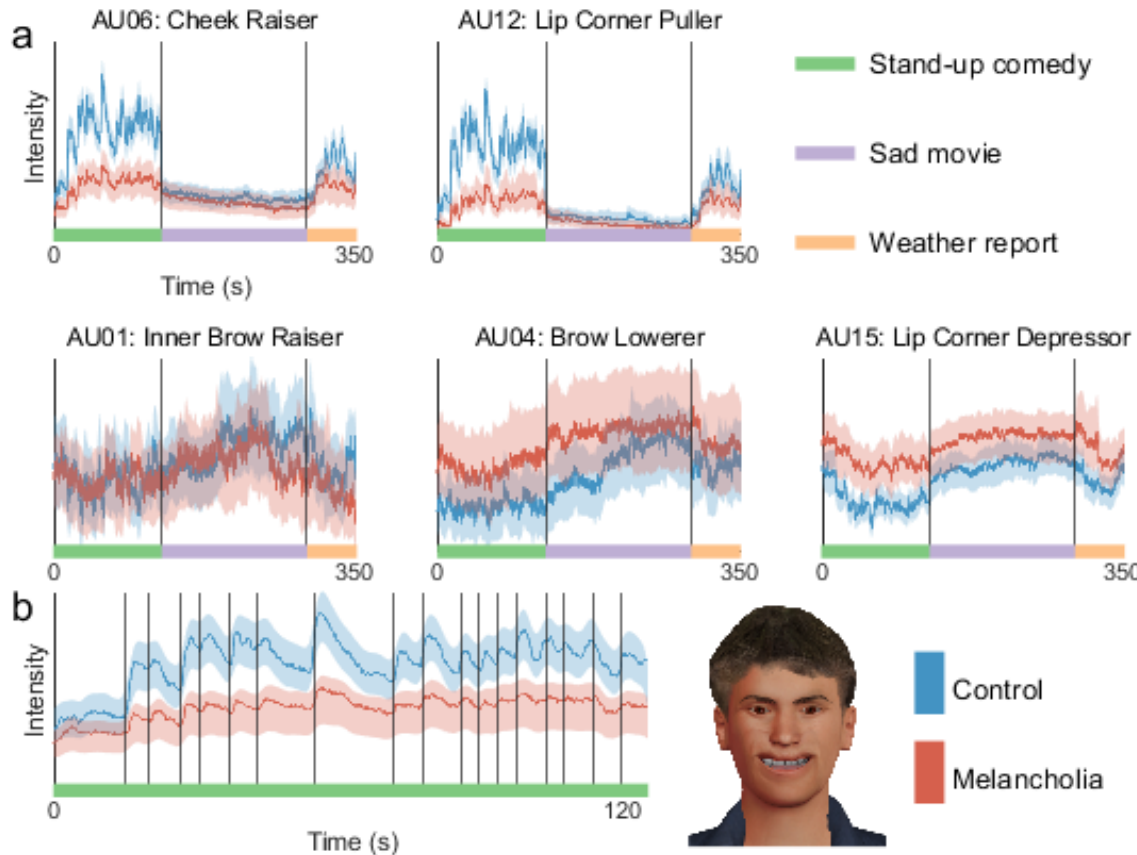
256 Group time courses in melancholia

257 Facial action unit time courses showed clear group differences (see Figure 3 for action units
258 typically implicated in expressing happiness and sadness, and Supplementary Figure 5 for all
259 action units). For each action unit in each participant, we calculated the median action unit
260 activation across each stimulus video. These were compared with a 3-way ANOVA, with
261 factors for clinical group, stimulus, and the facial valence. We considered two stimulus
262 videos, one with positive and one with negative valence, and two facial valence states,
263 happiness and sadness, calculated as sums of positively and negatively valenced action unit
264 activations respectively(8). A significant 3-way interaction was found between clinical group,
265 stimulus, and facial valence ($p=0.003$). Post-hoc comparisons with Tukey's honestly
266 significant difference criterion (Supplementary Figure 4) quantified that during stand-up
267 comedy, participants with melancholia had reduced activation of action unit 12 "Lip Corner
268 Puller" ($p<0.0001$) and increased activation of action unit 4 "Brow Lowerer" ($p<0.0001$).
269 Interestingly, facial responses of participants with melancholia during stand-up comedy, were
270 similar to those of controls during the sad movie ($p > 0.05$ for both action units).

271

272 To move away from individual action units, we next extracted the first principal component
273 across all action units. The time course of this composite component closely followed joke
274 punch lines during stand-up comedy (Figure 3b). This responsivity of this component to
275 movie events was substantially diminished in the melancholia cohort

276



277

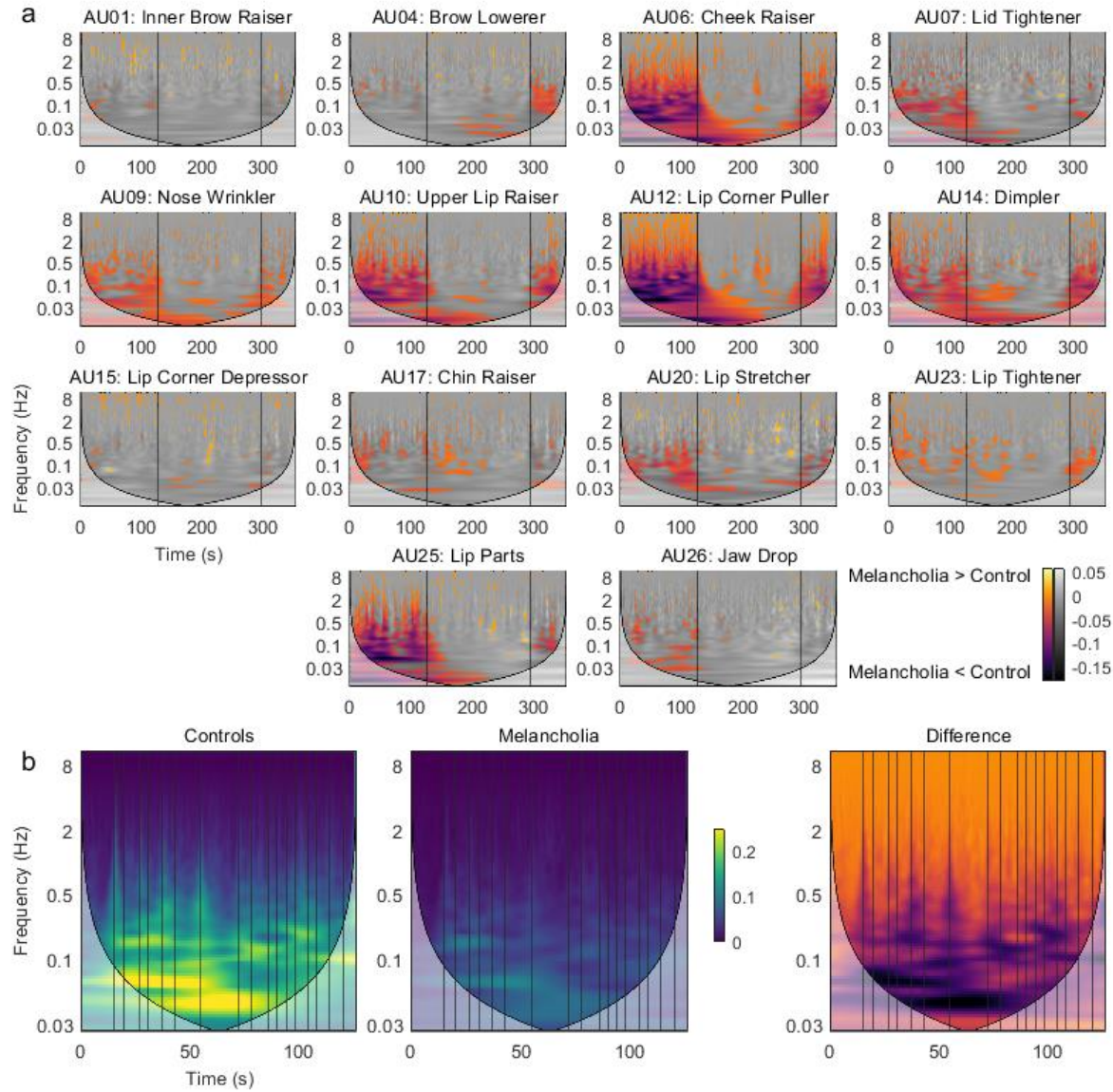
278 **Figure 3.** At each time point, mean intensity across participants of facial action unit
279 activation in controls (blue) and melancholia (red). Shading indicates 5% and 95%
280 confidence bands based on a bootstrap sample (n=100). (a) Action units commonly
281 implicated in happiness (top row) and sadness (bottom row). Participants watched stand-up
282 comedy, a sad video, and a funny video in sequence. Vertical lines demarcate transitions
283 between video clips. (b) First principal component of action units, shown during stand-up
284 comedy alone. Vertical lines indicate joke annotations. Avatar face shows the relative
285 contribution of each action unit to this component.

286

287 Time-frequency representation in melancholia

288 Time-frequency representations were calculated for all action units in all participants. For
289 each action unit, the mean time-frequency representation for the control group was subtracted
290 from the participants with melancholia (see Supplementary Figure 6 for the mean of the
291 controls). Significant group differences ($p < 0.05$) were found by comparison to a null
292 distribution composed of 100 resampled surrogate datasets (see Methods). Participants with
293 melancholia had a complex pattern of reduced activity encompassing a broad range of
294 frequencies (Figure 4a). The most prominent differences were in positive valence action units
295 during positive valence stimuli, but significant reductions were seen in most action units.

296 Differences in high frequency bands occurred during specific movie events such as jokes
297 (Figure 4b). There were sporadic instances of increased activity in melancholia participants
298 during the sad movie involving mainly action units 15 “Lip corner depressor” and 20 “Lip
299 stretcher”.



300
301 **Figure 4.** (a) Mean time-frequency activity in melancholia benchmarked to the control group.
302 Negative colour values (red-purple) indicate melancholia < controls ($p < 0.05$). Non-
303 significant group differences ($p > 0.05$) are indicated in greyscale. Vertical lines demarcate
304 stimulus videos. (b) Action unit 12 “Lip Corner Puller” during stand-up comedy in controls,
305 participants with melancholia, and difference between groups. Vertical lines indicate joke
306 annotations.

307

308 We next pursued whether the additional time-frequency information would improve the
309 classification accuracy of differentiating participants with melancholia from controls. A
310 support vector machine, using as inputs the mean action unit activation for each stimulus
311 video, achieved 63% accuracy with 5-fold cross-validation. In contrast, using as inputs the
312 mean time-frequency amplitude in discrete frequency bands within 0 – 5 Hz, improved
313 average cross-validation accuracy to 71%. As a control for the additional number of input
314 features, we tested a third set of models which naively modelled temporal dynamics using
315 mean action unit activations within shorter time blocks. These models had 63 – 64% accuracy
316 despite having a greater number of input features than the time-frequency representation
317 (Supplementary Table 3).

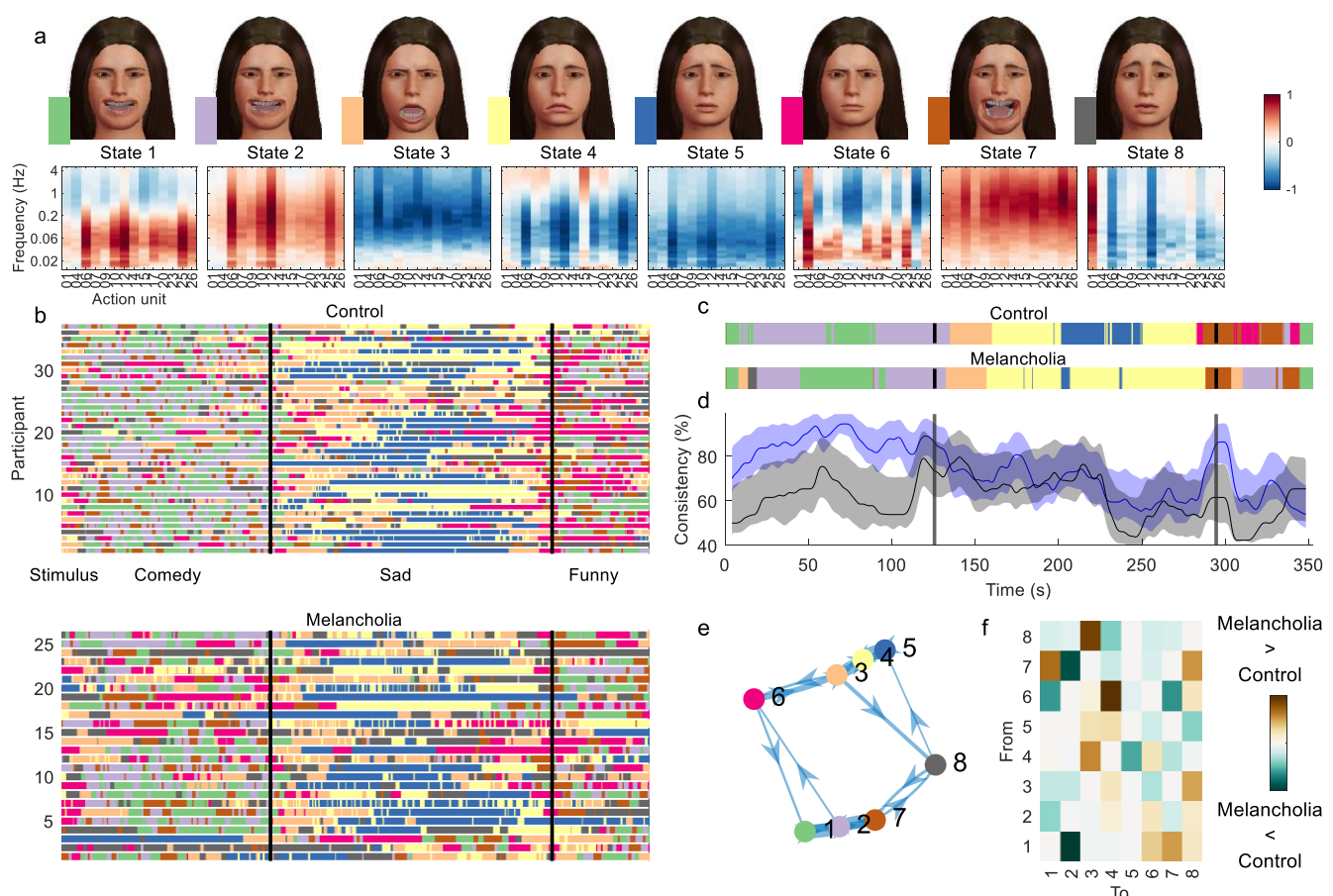
318

319 Sequential affective states in melancholia

320 Inverting a HMM from the time-frequency representations of facial action units yielded the
321 sequential expression of 8 states across participants (Figure 5).

- 322 • States 1 and 2 activated positive valence action units, each in distinct frequency bands,
323 and were dominant through the stand-up comedy for most participants (Figure 5B). State
324 2 comprised high frequency oscillations in positive valence action units, corresponding to
325 laughing or giggling.
- 326 • The sad movie was associated with early involvement of state 3, which deactivated high-
327 frequency activity, followed by states 4 and 5, which also deactivated oscillatory activity,
328 but with more specificity for lower frequencies and positive valence action units.
- 329 • State 6 comprised action units 4 “Brow Lowerer”, 9 “Nose Wrinkler”, 17 “Chin Raiser”,
330 and 23 “Lip Tightener”, traditionally associated with anger, disgust, or concern. State 7
331 can be associated with “gasping”, with very high frequency activation of most mouth-
332 associated action units including 25 “Lips Part”. These states occurred sporadically
333 through the weather report.
- 334 • State 8 predominantly activated action unit 1 “Inner Brow Raiser”, commonly associated
335 with negative valence.

336



337

338 **Figure 5.** Hidden Markov model inferred from time-frequency representation of melancholia
 339 dataset. (a) Contribution of action units and their spectral expression to each state. Avatar
 340 faces for each state show the relative contribution of each action unit. (b) State sequence for
 341 each participant at each time point, for controls (top) and participants with melancholia
 342 (bottom). Vertical lines demarcate stimulus clips. (c) Most common state across participants,
 343 using a 4s sliding temporal window. (d) Proportion of participants expressing the most
 344 common state for control (blue) and melancholia cohorts (black). Shading indicates 5% and
 345 95% bootstrap confidence bands. (e) Transition probabilities displayed as a weighted graph,
 346 with the top 20% of transition probabilities shown. States are positioned according to a force-
 347 directed layout where edge length is the inverse of transition probability. (f) Differences in
 348 mean transition probabilities between participants with melancholia and controls. Each
 349 row/column represents a HMM state. Colours indicate (melancholia – controls) values

350

351 The temporal sequence of most common states was similar across groups (Figure 5C), but the
 352 between-subjects consistency was markedly reduced in the melancholic participants during
 353 both funny videos (Figure 5D). Some participants with melancholia - for example
 354 participants 2 and 3 (Figure 5B) - had highly anomalous state sequences compared to other
 355 participants.

356

357 Fractional occupancy – the proportion of time spent by participants in each state – was
358 significantly different between groups for the positive valence states - state 1 (Melancholia <
359 Controls, $p_{FDR}=0.03$) and state 2 (Melancholia < Controls, $p_{FDR}=0.004$) – as well as for
360 negatively valenced state 8 (Melancholia > Controls $p_{FDR}=0.03$). We then asked whether
361 group differences in the time spent in each state were attributable to changes in the likelihood
362 of switching in to, or out of, specific facial states. Participants with melancholia were
363 significantly less likely to switch from a low-frequency positive valence state (1, smiling) to
364 high-frequency positive valence oscillations (state 2, giggling), but were more likely to
365 switch to states associated with any other emotion (states 4, 5, 6, 7, and 8). From the high
366 frequency positive valence state, they were more likely to switch to the deactivating “ennui”
367 state 4 (all $p_{FDR} < 0.05$).

368

369 **Discussion**

370

371 Facial expressions played a crucial role in the evolution of social intelligence in primates(2)
372 and continue to mediate human interactions. Observations of facial affect, its range and
373 reactivity play a central role in clinical settings. Quantitative analysis of facial expression has
374 accelerated of late, driven by methods to automatically factorise expressions into action
375 units(7) and the availability of large datasets of posed emotions(15). The dynamics of facial
376 expression mediate emotional reciprocity, but have received less attention(3). Naturalistic
377 stimuli offer distinct advantages to affective research for their ability to evoke these dynamic
378 responses(33), but their incompressibility has made analysis problematic. By leveraging
379 techniques in computer vision, we developed a pipeline to characterise facial dynamics
380 during naturalistic video stimuli. Analysis of healthy adults watching emotionally salient
381 videos showed that facial expression dynamics can be captured by a small number of
382 spatiotemporal states. These states co-activate facial muscle groups with a distinct spectral
383 fingerprint, and transition dynamically with the emotional context. Application of this
384 approach to melancholia showed that the clinical gestalt of facial non-reactivity in
385 melancholia(34) can be objectively identified not just with restrictions in spectral content, but
386 also with anomalous facial responses, more frequent occurrence of an ennui affect, and more
387 frequent state switching from transiently positive facial expressions to neutral and negative
388 states. This approach provides a unique perspective on how facial affect is generated by the
389 interplay between inner affective states and the sensorium.

390

391 Our pipeline first comprises automatic action unit extraction, then spectral wavelet-based
392 analysis of the ensuing feature dynamics. Wavelet energy at a given time corresponds to the
393 occurrence of a specific facial “event”, while energy in a given frequency reflects the
394 associated facial dynamics, like laughing. Unlike temporal averaging methods, which require
395 an arbitrary timescale, wavelets cover a range of timescales. The spectral approach also
396 allows participant facial responses to be pooled, without the limitations of averaging
397 responses whose phases are misaligned. We then inferred a hidden Markov model,
398 identifying spatially and spectrally resolved modes of dynamic facial activity which occur
399 sequentially with high consistency across participants viewing the same stimulus. States
400 transitions aligned with intuitive notions of affective transitions – for example, the common
401 transition between the low frequency and high frequency positive valence state, reflected
402 transitions between smiling and laughing.

403

404 Our method builds on the Emotion Facial Action Coding System (EMFACS)(8), where each
405 canonical emotion label (happy, angry, etc) is defined on the basis of a sparse set of
406 minimally necessary action units. The sparsity of this coding allows manual raters to find the
407 minimal necessary combinations of action units in a facial video to reflect an emotion label,
408 but may not include all action units that are involved in each affective state. Affective states
409 inferred from our HMM reflected prototypical action unit combinations from EMFACS, but
410 also provide a richer mapping across a broader range of action units. For example, while
411 happiness has been previously associated with just two action units, “Cheek Raiser” and “Lip
412 Corner Puller”, such sparse activations are rare, particularly during intense emotional
413 displays. We demonstrated that laughing during stand-up comedy activated eyebrow-related
414 action units, some of which are traditionally associated with sadness. Conversely, negatively
415 valenced stimuli dampened facial movements, with a relative sparing of those action units
416 typically associated with sadness.

417

418 Ensembles of HMMs have previously been used to improve emotion classification accuracy
419 when benchmarked against manually coded datasets. In these studies, one HMM models the
420 temporal dynamics of one action unit(35,36) or one universal basic emotion(13,37), with
421 HMM states corresponding to expression onset/offset. Given a video frame, the HMM with
422 the greatest evidence determines the decoded expression. Nested HMMs have also been
423 employed, with a second level HMM predicted transitions between the basic emotions(38). In

424 contrast, the present method uses a single HMM to describe facial expressions without prior
425 emotion categories, capturing the dynamic co-occurrence of facial actions that together
426 comprise distinct affective states. By taking the spectral activity of action units as input
427 features into the HMM, our approach uniquely captures the spatiotemporal texture of
428 naturally occurring facial affect. This enables, for example, the disambiguation of a smile
429 from a giggle. The importance of the spectral characterization is highlighted by our finding
430 that in melancholia, smile states were more likely to transition to ennui, and less likely to the
431 laughter state. Our use of dynamic spectra as inputs into a HMM is similar to their recent use
432 in neuroimaging research(39). Using the raw time series is also possible – hence additionally
433 capturing phase relationships, although this comes with an additional computational burden
434 and reduced interpretability of states(40).

435

436 Dynamic facial patterns were influenced by the affective properties of the stimulus video. For
437 the DISFA dataset, the HMM inferred two disgust-associated states, in low and high
438 frequency bands respectively. These states occurred predominantly during two disgusting
439 video clips. For the melancholia dataset, the inferred HMM states over-represented happiness
440 and sadness, and under-represented disgust. This is ostensibly because the stimulus had
441 prominent positive and negatively valenced sections without disgusting content. The co-
442 occurrence of the states and the state transitions across participants speaks to the influence of
443 the video content on affective responses and hence, more broadly, the dynamic exchange
444 between facial affect and the social environment.

445

446 We found that participants with melancholia exhibited broad reductions in facial activity, as
447 well as specific reductions in high frequency activity in response to specific events such as
448 joke punchlines, reflecting the clinical gestalt of impaired affective reactivity(30). Viewing
449 affect as a dynamic process provided two further insights into facial responses in
450 melancholia. First, decreased between-subject consistency and more anomalous facial
451 responses suggest that their facial activity is less likely to be driven by a common external
452 stimulus. Ambiguous facial responses are also seen in schizophrenia(41), suggesting the
453 possibility of a common underlying mechanism with melancholia. Second, participants with
454 melancholia were less likely to enter high frequency positive valence states like laughing, and
455 once there, transitioned out quickly to the “ennui” state. This reflects the clinical impression
456 that positive mood states persist in healthy controls, but such states are fleeting in those with
457 melancholia, who tend to get “stuck” in negative mood states instead. The results are

458 commensurate with the proposal that depressed states relate to persistent firing in non-reward
459 functional areas mediated by attractor dynamics(42). Additionally, these findings accord with
460 neurobiological models of melancholia whereby dysfunctional cortical-basal ganglia circuitry
461 underlie the disturbances in volition and psychomotor activity that characterise the
462 disorder(30). More generally, the notion of affect as a sequence of spatiotemporal states
463 aligns with the proposal that instabilities in brain network activity generate adaptive
464 fluctuations in mood and affect, with these being either over- or under-damped in affective
465 disorders(43). Our paradigm also raises clinical questions predicated on dynamics – for
466 example, do biological or psychological treatments for melancholia work by increasing the
467 probability of entering positive affective states, or reducing the probability of exiting such
468 states?

469

470 Several caveats bear mention. First, a small number of participants with constant zero
471 activation in one or more action units were excluded from analysis, because this produces an
472 ill-defined spectral transform. Excluded participants, of whom 1 was a control and 4 had
473 melancholia, may have had the greatest impairments in facial affect. This issue could be
474 addressed with a lower detectable limit of action unit activation. Second, time-frequency
475 maps were standardised in mean and variance before HMM inference. This ensures that states
476 occur sequentially across time, but reduces the differences in state sequences across groups.
477 Omitting this standardisation step yields states that are biased towards group differences
478 rather than temporal differences (see Supplementary Figure 7). Future work could consider
479 methods that are less susceptible to this trade-off. Finally, the utility of our approach is likely
480 to be improved by multimodal fusion of facial, head pose, vocal and body language
481 behaviour, each of which independently improve classification(44–47).

482

483 Human emotion and affect are inherently dynamic. Our work demonstrates that momentary
484 affective responses, such as laughing or grimacing, traditionally viewed from a qualitative
485 standpoint, can be understood within a quantitative framework. These tools provide a
486 translational platform for mental health research to understand the dynamics of facial affect -
487 for example in clinical states such as melancholia with its distinctive sign of psychomotor
488 disturbance, the masked facies of Parkinson’s disease, emotional incongruence and affective
489 blunting in schizophrenia, and emotional lability integral to bipolar disorder.

490

491

492
493
494
495
496

497 **Materials and Methods**

498 Data

499 The Denver Intensity of Spontaneous Facial Action (DISFA) dataset contains facial videos
500 recorded at 20 frames per second from 27 participants who viewed a 4 minute video
501 consisting of short emotive clips from Youtube(19) (Supplementary Table 1).

502

503 The melancholia dataset comprises 30 participants with major depressive disorder, who were
504 recruited from the specialist depression clinic at the Black Dog Institute in Sydney, Australia.
505 These participants met criteria for a current major depressive episode, were diagnosed as
506 having the melancholic subtype by previously detailed criteria(48), and did not have lifetime
507 (hypo)mania or psychosis (Table 1). 38 matched healthy controls were recruited from the
508 community. All participants were screened for psychotic and mood conditions with the Mini
509 International Neuropsychiatric Interview (MINI). Exclusion criteria were current or past
510 substance dependence, recent electroconvulsive therapy, neurological disorder, brain injury,
511 invasive neurosurgery, or an estimated full scale IQ score (WAIS-III) below 80. Participants
512 provided informed consent for the study. Participants watched 3 video clips consecutively –
513 stand-up comedy (120 seconds), a sad movie clip (152 seconds), and a German weather
514 report video depicting a weather reporter laughing uncontrollably (56 seconds). Facial video
515 was recorded at a resolution of 800 x 600 pixels at 25 frames per second using an AVT Pike
516 F-100 FireWire camera. The camera was mounted on a tripod, which was placed behind the
517 monitor so as to record the front of the face. The height of the camera was adjusted with
518 respect to the participant's height when seated.

519

520 **Table 1.** Demographics and clinical characteristics

521

| | Healthy controls | Melancholia | Group comparison, <i>t</i> or χ^2 , p-value |
|------------------------|------------------|-------------|---|
| Number of participants | 38 | 30 | - |
| Age, mean (SD) | 46.5 (20.0) | 46.2 (15.5) | 0.95 |

| | | | |
|--|----------|----------|------|
| Sex (M:F) | 13:19 | 17:13 | 0.21 |
| Medication, % yes (n) | | | |
| Any psychiatric medication | 7% (1) | 85% (23) | - |
| Nil medication | 93% (13) | 15% (4) | - |
| Selective serotonin reuptake inhibitor | 7% (1) | 15% (4) | - |
| Dual-action antidepressant ^a | 0% (0) | 48% (13) | - |
| Tricyclic or monoamine oxidase inhibitor | 0% (0) | 19% (5) | - |
| Mood stabilizer ^b | 0% (0) | 11% (3) | - |
| Antipsychotic | 0% (0) | 33% (9) | - |

522 ^a For example, serotonin noradrenaline reuptake inhibitor

523 ^b For example, lithium or valproate

524

525 Facial action units

526 For the melancholia dataset, facial video recordings of different participants were aligned
527 with FaceSync(49). For both datasets, facial action unit intensities were extracted with
528 OpenFace(31). OpenFace uses a convolutional neural network architecture, Convolutional
529 Experts Constrained Local Model (CE-CLM), to detect and track facial landmark points.
530 After face images are aligned to a common 112 x 112 pixel image, histogram of oriented
531 gradients features are extracted. A linear kernel support vector machine was then trained on 6
532 facial expression datasets with manually coded action unit occurrence times.

533

534 Action unit time series from OpenFace for each participant were not normalised, as we were
535 interested in between-subjects differences. Recordings with more than 0.5% missing frames
536 were excluded, and any remaining missing frames were linearly interpolated. Action unit 45
537 “Blink” was not used as it is not directly relevant to emotion. Action units 2 “Outer Brow
538 Raiser” and 5 “Upper Lid Raiser” were not used as they had constant zero value throughout
539 the recording for most participants. Participants with any other action units with zero value
540 through the recording were also excluded, as the time-frequency representation is undefined
541 for these time series. This comprised 1 control and 4 participants with melancholia.

542

543 Time-frequency representation

544 For each participant, each facial action unit time series was transformed into a time-frequency
545 representation, using the amplitude of the continuous wavelet transform. An analytic Morse
546 wavelet was used with symmetry parameter 3, time-bandwidth product 60, and 12 voices per
547 octave. Mean time-frequency maps were visualised with a cone of influence – outside which
548 edge effects produce artefact (Supplementary Figure 2 for DISFA, Supplementary Figure 6
549 for melancholia dataset). To determine information lost by averaging raw time series across
550 participants, the amplitude of the continuous wavelet transform for the group mean time
551 series was calculated. At each point in time-frequency space, the distribution of individual
552 participants' amplitude was compared with the amplitude of the group mean, with a two-
553 sided t-test ($p=0.05$) (Figure 1).

554

555 Hidden Markov model

556 A Hidden Markov model (HMM), implemented in the HMM-MAR MATLAB toolbox
557 (<https://github.com/OHBA-analysis/HMM-MAR>)(50), was used to identify states
558 corresponding to oscillatory activity localised to specific action units and frequency bands. A
559 HMM specifies state switching probabilities which arise from a time-invariant transition
560 matrix. Each state is described by a multivariate Gaussian observation model with distinct
561 mean and covariance in (action unit x frequency) space. Input data were 110 frequency bins
562 in 0-5Hz, for each of 14 facial action units. Individual participants' time series were
563 standardised to zero mean and unit variance before temporal concatenation to form a single
564 time series. This time series was downsampled to 10Hz, and the top 10 principal components
565 were used (for DISFA). Other HMM parameters are listed in Supplementary Table 4.

566

567 The initialisation algorithm used 10 optimisation cycles per repetition. Variational model
568 inference optimised free energy, a measure of model accuracy penalised by model
569 complexity, and stopped after the relative decrement in free energy dropped below 10^{-5} . Free
570 energy did not reach a minimum even beyond $n=30$ states (Supplementary Figure 3).
571 Previous studies have chosen between 5 and 12 states(51,52). We chose an 8-state model as
572 done in previous work(39), as visual inspection of the states showed trivial splitting of states
573 beyond this value. However, the analyses were robust to variations in the exact number of
574 states.

575

576 HMM state observation models were visualised with FACSHuman(53). The contribution of
577 each action unit to each state was calculated by summing across all frequency bands. For
578 each state, positive contributions were rescaled to the interval [0,1] and visualised on an
579 avatar face (Figure 2a). State sequences for individual subjects were calculated with the
580 Viterbi algorithm (Figure 2). To calculate between-subjects consistency of state sequences
581 over time, we used an 8s sliding window. Within this window, for each state, we counted the
582 number of participants who expressed this state at least once, and found the most commonly
583 expressed state. Uncertainty in this consistency measure at each time point was estimated
584 from the 5 and 95 percentiles of 100 bootstrap samples. The null distribution for consistency
585 was obtained by randomly circular shifting the Viterbi time series for each subject
586 independently (n=100). Consistency values exceeding the 95th percentile (59% consistency)
587 were deemed significant.

588

589 Analysis of melancholia dataset

590 Mean action unit activations were calculated for each group, and uncertainty visualised with
591 the 5th and 95th percentiles of 100 bootstrap samples (Figure 3, Supplementary Figure 5). A
592 3-way ANOVA for activation was conducted with group, stimulus video, and facial valence
593 as regressors. To avoid redundancy between the two positive valence videos, we limited the
594 ANOVA to two stimulus videos – the stand-up comedy and sad movie clips. In keeping with
595 previous work(8), we defined happiness as the sum of action units 6 “Cheek Raiser” and 12
596 “Lip Corner Puller”, and sadness as the sum of action units 1 “Inner Brow Raiser”, 4 “Brow
597 Lowerer”, and 15 “Lip Corner Depressor”. Post-hoc comparisons used Tukey’s honestly
598 significant difference criterion (Supplementary Figure 4).

599

600 Time-frequency representations were computed as the amplitude of the continuous wavelet
601 transform. Group differences in wavelet power, localised in time and frequency, were
602 calculated by subtracting the mean time-frequency representation of each clinical group
603 (Figure 4). To confirm that these effects were not due to movement-related noise in action
604 unit encoding having different effects depending on the frequency and time window
605 considered, the null distribution of the effect was obtained by resampling 100 surrogate
606 cohorts from the list of all participants. Time-frequency points with effect size inside 2.5 –
607 97.5 percentile were considered non-significant and excluded from visualisation.

608

609 To compare classification accuracy with action unit time series or time-frequency data, a
610 support vector machine with Gaussian kernel was used. All tests used mean accuracy over 5
611 repetitions of 5-fold cross validation, but varied in the input features. Inputs to the first model
612 were mean action unit activations for each action unit (n=14) and each stimulus video (n=3).
613 For the time-frequency model, inputs were mean wavelet amplitude in each frequency bin
614 (n=10) in each stimulus video, for each action unit. For the third set of models, input features
615 were mean action unit activation within discrete time chunks of 2, 10, and 30 seconds
616 (Supplementary Table 3).

617

618 The HMM was inferred as described above (Figure 5). Supplementary Figure 7 shows the
619 results when input data were not standardised. Local transition probabilities were then
620 inferred for each participant separately. Two-sided significance testing for group differences
621 in fractional occupancy was implemented within the HMM-MAR toolbox by permuting
622 between subjects as described previously(54). Next, we considered only those state
623 transitions that could explain the group differences in fractional occupancy and tested these
624 transitions for group differences with t-tests (one-sided in the direction that could explain
625 fractional occupancy findings). Group differences in fractional occupancy and transition
626 probability were corrected to control the false discovery rate(55).

627

628 Results were consistent across repetitions of HMM inference with different initial random
629 seeds. In addition, all analyses were repeated with time-frequency amplitudes normalised by
630 the standard deviation of the time series, to ensure that results were not solely due to group
631 differences in variance for each action unit time. This was motivated by previous work
632 showing that the square of wavelet transform amplitude increases with variance for white
633 noise sources(56). Results were consistent with and without normalisation, including
634 differences between clinical groups, the distributions and time courses of HMM states.

635

636 **Acknowledgements**

637 JJ acknowledges the support of a Health Education & Training Institute Award in Psychiatry
638 and Mental Health, and the Rainbow Foundation. MB acknowledges the support of the
639 National Health and Medical Research Council (1118153, 10371296, 1095227) and the
640 Australian Research Council (CE140100007).

641

642

643 **Data availability**

644 The DISFA dataset is publically available at <http://mohammadmahoor.com/disfa/>. The
645 melancholia dataset is not publically available due to ethical and privacy considerations for
646 patients.

647

648

649 **Code availability**

650 Code to replicate the analysis of healthy controls in the DISFA dataset is available at
651 <https://github.com/jaysonjeg/FacialDynamicsHMM>

652

653

654 **References**

655

- 656 1. Naumann LP, Vazire S, Rentfrow PJ, Gosling SD. Personality Judgments Based on Physical
657 Appearance. *Pers Soc Psychol Bull*. 2009 Dec 1;35(12):1661–71.
- 658 2. SCHMIDT KL, COHN JF. Human Facial Expressions as Adaptations: Evolutionary Questions in
659 Facial Expression Research. *Am J Phys Anthropol*. 2001;Suppl 33:3–24.
- 660 3. Ambadar Z, Schooler JW, Cohn JF. Deciphering the Enigmatic Face: The Importance of Facial
661 Dynamics in Interpreting Subtle Facial Expressions. *Psychol Sci*. 2005 May 1;16(5):403–10.
- 662 4. Ekman P. Are there basic emotions? *Psychol Rev*. 1992 Jul;99(3):550–3.
- 663 5. Ortony A. Are All ‘Basic Emotions’ Emotions? A Problem for the (Basic) Emotions Construct.
664 *Perspect Psychol Sci J Assoc Psychol Sci*. 2022 Jan;17(1):41–61.
- 665 6. Keltner D, Sauter D, Tracy J, Cowen A. Emotional Expression: Advances in Basic Emotion
666 Theory. *J Nonverbal Behav*. 2019 Jun;43(2):133–60.
- 667 7. Ekman P, Friesen WV, Friesen WV, Hager J. Facial action coding system: A technique for the
668 measurement of facial movement. 1978 Jan 1 [cited 2020 Apr 15]; Available from:
669 <https://www.scienceopen.com/document?vid=759f6f74-7ccd-47b5-904a-25ca0f29ea90>
- 670 8. Friesen WV, Ekman P. EMFACS-7: Emotional Facial Action Coding System. Version 7. 1983.
- 671 9. Feng X. Facial expression recognition based on local binary patterns and coarse-to-fine
672 classification. In: The Fourth International Conference on Computer and Information
673 Technology, 2004 CIT ’04. 2004. p. 178–83.
- 674 10. Kumar P, Happy SL, Routray A. A real-time robust facial expression recognition system using
675 HOG features. In: 2016 International Conference on Computing, Analytics and Security Trends
676 (CAST). 2016. p. 289–93.

677 11. Tian Y li, Kanade T, Cohn JF. Recognizing Action Units for Facial Expression Analysis. *IEEE Trans*
678 *Pattern Anal Mach Intell.* 2001 Feb;23(2):97–115.

679 12. Ghimire D, Lee J. Geometric Feature-Based Facial Expression Recognition in Image Sequences
680 Using Multi-Class AdaBoost and Support Vector Machines. *Sensors.* 2013 Jun;13(6):7714–34.

681 13. Yeasin M, Bullet B, Sharma R. Recognition of facial expressions and measurement of levels of
682 interest from video. *IEEE Trans Multimed.* 2006 Jun;8(3):500–8.

683 14. Ekundayo O, Viriri S. Facial Expression Recognition: A Review of Methods, Performances and
684 Limitations. In: 2019 Conference on Information Communications Technology and Society
685 (ICTAS). 2019. p. 1–6.

686 15. Lucey P, Cohn JF, Kanade T, Saragih J, Ambadar Z, Matthews I. The Extended Cohn-Kanade
687 Dataset (CK+): A complete dataset for action unit and emotion-specified expression. In: 2010
688 IEEE Computer Society Conference on Computer Vision and Pattern Recognition - Workshops.
689 2010. p. 94–101.

690 16. Darzi A, Provenza NR, Jeni LA, Borton DA, Sheth SA, Goodman WK, et al. Facial Action Units and
691 Head Dynamics in Longitudinal Interviews Reveal OCD and Depression severity and DBS
692 Energy. In: 2021 16th IEEE International Conference on Automatic Face and Gesture
693 Recognition (FG 2021). 2021. p. 1–6.

694 17. Lang P, Bradley M, Cuthbert B. International affective picture system (IAPS): Affective ratings of
695 pictures and instruction manual. Technical Report A-8. University of Florida, Gainesville, FL;
696 2008.

697 18. Kollias D, Tzirakis P, Nicolaou MA, Papaioannou A, Zhao G, Schuller B, et al. Deep Affect
698 Prediction in-the-Wild: Aff-Wild Database and Challenge, Deep Architectures, and Beyond. *Int J*
699 *Comput Vis.* 2019 Jun 1;127(6):907–29.

700 19. Mavadati SM, Mahoor MH, Bartlett K, Trinh P, Cohn JF. DISFA: A Spontaneous Facial Action
701 Intensity Database. *IEEE Trans Affect Comput.* 2013 Apr;4(2):151–60.

702 20. Soleymani M, Lichtenauer J, Pun T, Pantic M. A Multimodal Database for Affect Recognition
703 and Implicit Tagging. *IEEE Trans Affect Comput.* 2012 Jan;3(1):42–55.

704 21. Sonkusare S, Breakspear M, Guo C. Naturalistic Stimuli in Neuroscience: Critically Acclaimed.
705 *Trends Cogn Sci.* 2019 Aug 1;23(8):699–714.

706 22. Schultz J, Pilz KS. Natural facial motion enhances cortical responses to faces. *Exp Brain Res Exp*
707 *Hirnforsch Exp Cerebrale.* 2009 Apr;194(3):465–75.

708 23. Cohn JF, Kruez TS, Matthews I, Yang Y, Nguyen MH, Padilla MT, et al. Detecting depression
709 from facial actions and vocal prosody. In: 2009 3rd International Conference on Affective
710 Computing and Intelligent Interaction and Workshops. 2009. p. 1–7.

711 24. Gavrilescu M, Vizireanu N. Predicting Depression, Anxiety, and Stress Levels from Videos Using
712 the Facial Action Coding System. *Sensors.* 2019 Jan;19(17):3693.

713 25. Dibeklioğlu H, Hammal Z, Yang Y, Cohn JF. Multimodal Detection of Depression in Clinical
714 Interviews. *Proc ACM Int Conf Multimodal Interact ICMI Conf.* 2015 Nov;2015:307–10.

715 26. Bhatia S, Hayat M, Breakspear M, Parker G, Goecke R. A Video-Based Facial Behaviour Analysis
716 Approach to Melancholia. In: 2017 12th IEEE International Conference on Automatic Face
717 Gesture Recognition (FG 2017). 2017. p. 754–61.

718 27. Renneberg B, Heyn K, Gebhard R, Bachmann S. Facial expression of emotions in borderline
719 personality disorder and depression. *J Behav Ther Exp Psychiatry*. 2005 Sep 1;36(3):183–96.

720 28. Tréneau F, Malaspina D, Duval F, Corrêa H, Hager-Budny M, Coin-Bariou L, et al. Facial
721 Expressiveness in Patients With Schizophrenia Compared to Depressed Patients and
722 Nonpatient Comparison Subjects. *Am J Psychiatry*. 2005 Jan 1;162(1):92–101.

723 29. Girard JM, Cohn JF, Mahoor MH, Mavadati SM, Hammal Z, Rosenwald DP. Nonverbal social
724 withdrawal in depression: Evidence from manual and automatic analyses. *Image Vis Comput*.
725 2014 Oct 1;32(10):641–7.

726 30. Parker G, Hadzi-Pavlovic D, Evers K, editors. *Melancholia: a disorder of movement and mood: a*
727 *phenomenological and neurobiological review*. Cambridge University Press; 1996.

728 31. Baltrusaitis T, Zadeh A, Lim YC, Morency L. OpenFace 2.0: Facial Behavior Analysis Toolkit. In:
729 2018 13th IEEE International Conference on Automatic Face & Gesture Recognition. Xi'an,
730 China; 2018. p. 59–66.

731 32. Guo CC, Hyett MP, Nguyen VT, Parker GB, Breakspear MJ. Distinct neurobiological signatures of
732 brain connectivity in depression subtypes during natural viewing of emotionally salient films.
733 *Psychol Med*. 2016 May;46(7):1535–45.

734 33. Dhall A, Goecke R, Lucey S, Gedeon T. Collecting Large, Richly Annotated Facial-Expression
735 Databases from Movies. *IEEE Multimed*. 2012 Jul;19(3):34–41.

736 34. Parker G. Defining melancholia: the primacy of psychomotor disturbance. *Acta Psychiatr Scand*
737 *Suppl*. 2007;(433):21–30.

738 35. Jiang B, Valstar M, Martinez B, Pantic M. A Dynamic Appearance Descriptor Approach to Facial
739 Actions Temporal Modeling. *IEEE Trans Cybern*. 2014 Feb;44(2):161–74.

740 36. Koelstra S, Pantic M, Patras I. A Dynamic Texture-Based Approach to Recognition of Facial
741 Actions and Their Temporal Models. *IEEE Trans Pattern Anal Mach Intell*. 2010
742 Nov;32(11):1940–54.

743 37. Sandbach G, Zafeiriou S, Pantic M, Rueckert D. Recognition of 3D facial expression dynamics.
744 *Image Vis Comput*. 2012 Oct;30(10):762–73.

745 38. Cohen I, Sebe N, Garg A, Chen LS, Huang TS. Facial expression recognition from video
746 sequences: temporal and static modeling. *Comput Vis Image Underst*. 2003 Jul 1;91(1):160–87.

747 39. Baker AP, Brookes MJ, Rezek IA, Smith SM, Behrens T, Probert Smith PJ, et al. Fast transient
748 networks in spontaneous human brain activity. *eLife*. 2014 Mar 25;3:e01867.

749 40. Vidaurre D, Hunt LT, Quinn AJ, Hunt BAE, Brookes MJ, Nobre AC, et al. Spontaneous cortical
750 activity transiently organises into frequency specific phase-coupling networks. *Nat Commun*.
751 2018 Jul 30;9(1):2987.

752 41. Hamm J, Pinkham A, Gur RC, Verma R, Kohler CG. Dimensional information-theoretic
753 measurement of facial emotion expressions in schizophrenia. *Schizophr Res Treat*.
754 2014;2014:243907.

755 42. Rolls ET. A non-reward attractor theory of depression. *Neurosci Biobehav Rev*. 2016 Sep
756 1;68:47–58.

757 43. Perry A, Roberts G, Mitchell PB, Breakspear M. Connectomics of bipolar disorder: a critical
758 review, and evidence for dynamic instabilities within interoceptive networks. *Mol Psychiatry*.
759 2019 Sep;24(9):1296–318.

760 44. Bhatia S, Hayat M, Goecke R. A multimodal system to characterise melancholia: cascaded bag
761 of words approach. In: Proceedings of the 19th ACM International Conference on Multimodal
762 Interaction [Internet]. New York, NY, USA: Association for Computing Machinery; 2017 [cited
763 2020 Sep 8]. p. 274–80. (ICMI '17). Available from: <http://doi.org/10.1145/3136755.3136766>

764 45. Alghowinem S, Goecke R, Wagner M, Parkex G, Breakspear M. Head Pose and Movement
765 Analysis as an Indicator of Depression. In: 2013 Humaine Association Conference on Affective
766 Computing and Intelligent Interaction. 2013. p. 283–8.

767 46. Alghowinem S, Goecke R, Wagner M, Epps J, Breakspear M, Parker G. Detecting depression: A
768 comparison between spontaneous and read speech. In: 2013 IEEE International Conference on
769 Acoustics, Speech and Signal Processing. 2013. p. 7547–51.

770 47. Joshi J, Goecke R, Parker G, Breakspear M. Can body expressions contribute to automatic
771 depression analysis? In: 2013 10th IEEE International Conference and Workshops on Automatic
772 Face and Gesture Recognition (FG). 2013. p. 1–7.

773 48. Taylor MA, Fink M. Melancholia: The diagnosis, pathophysiology, and treatment of depressive
774 illness. New York, NY, US: Cambridge University Press; 2006. xiv, 544 p. (Melancholia: The
775 diagnosis, pathophysiology, and treatment of depressive illness).

776 49. Cheong JH, Brooks S, Chang L. FaceSync: Open source framework for recording facial
777 expressions with head-mounted cameras. 2017.

778 50. Vidaurre D, Quinn AJ, Baker AP, Dupret D, Tejero-Cantero A, Woolrich MW. Spectrally resolved
779 fast transient brain states in electrophysiological data. *NeuroImage*. 2016 Feb 1;126:81–95.

780 51. Vidaurre D, Smith SM, Woolrich MW. Brain network dynamics are hierarchically organized in
781 time. *Proc Natl Acad Sci*. 2017 Nov 28;114(48):12827–32.

782 52. Kottaram A, Johnston LA, Cocchi L, Ganella EP, Everall I, Pantelis C, et al. Brain network
783 dynamics in schizophrenia: Reduced dynamism of the default mode network. *Hum Brain Mapp*.
784 2019 May;40(7):2212–28.

785 53. Gilbert M, Demarchi S, Urdapilleta I. FACSHuman, a software program for creating
786 experimental material by modeling 3D facial expressions. *Behav Res Methods*. 2021 Oct
787 1;53(5):2252–72.

788 54. Vidaurre D, Woolrich MW, Winkler AM, Karapanagiotidis T, Smallwood J, Nichols TE. Stable
789 between-subject statistical inference from unstable within-subject functional connectivity
790 estimates. *Hum Brain Mapp*. 2019;40(4):1234–43.

791 55. Storey JD. A direct approach to false discovery rates. *J R Stat Soc Ser B Stat Methodol.*
792 2002;64(3):479–98.

793 56. Torrence C, Compo GP. A Practical Guide to Wavelet Analysis. *Bull Am Meteorol Soc.*
794 1998;79(1):18.

795